Appl Microbiol Biotechnol (2016) 100:3347–3360
DOI 10.1007/s00253-015-7106-z

ENVIRONMENTAL BIOTECHNOLOGY

Comparison of bacterial and archaeal communities in depth-resolved zones in an LNAPL body

Maria Irianni-Renno[2] · Daria Akhbari[2,4] · Mitchell R. Olson[2,5] · Adam P. Byrne[2,6] · Emilie Lefèvre[2,7] · Julio Zimbron[2] · Mark Lyverse[3] · Thomas C. Sale[2] · Susan K. De Long[1]

Received: 12 August 2015 / Revised: 13 October 2015 / Accepted: 15 October 2015 / Published online: 22 December 2015

Abstract Advances in our understanding of the microbial ecology at sites impacted by light non-aqueous phase liquids (LNAPLs) are needed to drive development of optimized bioremediation technologies, support longevity models, and develop culture-independent molecular tools. In this study, depth-resolved characterization of geochemical parameters and microbial communities was conducted for a shallow hydrocarbon-impacted aquifer. Four distinct zones were identified based on microbial community structure and geochemical data: (i) an aerobic, low-contaminant mass zone at the top of the vadose zone; (ii) a moderate to high-contaminant mass, low-oxygen to anaerobic transition zone in the middle of the vadose zone; (iii) an anaerobic, high-contaminant mass zone spanning the bottom of the vadose zone and saturated zone; and (iv) an anaerobic, low-contaminant mass zone below the LNAPL body. Evidence suggested that hydrocarbon degradation is mediated by syntrophic fermenters and methanogens in zone III. Upward flux of methane likely contributes to promoting anaerobic conditions in zone II by limiting downward flux of oxygen as methane and oxygen fronts converge at the top of this zone. Observed sulfate gradients and microbial communities suggested that sulfate reduction and methanogenesis both contribute to hydrocarbon degradation in zone IV. Pyrosequencing revealed that *Syntrophus*- and *Methanosaeta*-related species dominate bacterial and archaeal communities, respectively, in the LNAPL body below the water table. Observed phylotypes were linked with in situ anaerobic hydrocarbon degradation in LNAPL-impacted soils.

Keywords Biodegradation · LNAPL · Petroleum hydrocarbons · Microbial communities · Pyrosequencing

Electronic supplementary material The online version of this article (doi:10.1007/s00253-015-7106-z) contains supplementary material, which is available to authorized users.

✉ Susan K. De Long
susan.de_long@colostate.edu

[1] Department of Civil and Environmental Engineering, Colorado State University, 1301 Campus Delivery, Fort Collins, CO 80523, USA

[2] Department of Civil and Environmental Engineering, Colorado State University, 1320 Campus Delivery, Fort Collins, CO 80523, USA

[3] Chevron Energy Technology Company, 6001 Bollinger Canyon Road, Bldg. C1206, San Ramon, CA 94583, USA

[4] Present address: Department of Geological Sciences, Jackson School of Geosciences, University of Texas at Austin, Austin, TX 78712, USA

[5] Present address: Trihydro Corporation, Fort Collins, CO 80524, USA

[6] Present address: Department of Civil and Environmental Engineering, University of California, 209 O'Brien Hall, Berkeley, CA 94720, USA

[7] Present address: Department of Civil and Environmental Engineering, Duke University, 121 Hudson Hall, Box 90287, Durham, NC 27708, USA

Introduction

Standard practices over the last century have commonly led to subsurface petroleum hydrocarbon releases (Sale 2003). and current worldwide releases of crude oil to the environment have been estimated to be 400,000 to 800,000 metric tons per year (Das and Chandran 2010). In the subsurface, light non-aqueous phase liquid (LNAPL) zones act as sources of aqueous and vapor phase plumes containing contaminants including benzene, toluene, ethylbenzene, and xylenes (BTEXs) (Landmeyer et al. 1998; Newman et al. 1991). In the absence of remedial actions that directly target LNAPL, LNAPL source zones can persist at contaminated sites for decades causing continuing threats to groundwater quality (Huntley and Beckett

2002) and/or indoor air (Roggemans et al. 2001). Remediation of LNAPL source zones is critical to managing risks posed by subsurface hydrocarbon contamination (Chadalavada et al. 2012). Unfortunately, widely used technologies such as hydraulic recovery are only effective for the mobile LNAPL fraction and leave large amounts of immobile (residual) LNAPL in source zones (Sale 2003). New technologies and/or strategies are needed to manage residual LNAPL present after active remediation and/or extended periods of natural depletion.

Microbially based treatment technologies, such as monitored natural attenuation (MNA), are popular for treatment of hydrocarbon plumes because these technologies are often effective, relatively inexpensive, and minimally invasive (Declercq et al. 2012; Jørgensen et al. 2010). Historically, the applicability of MNA, or other microbially based treatments, to LNAPL source zones has been considered questionable because biodegradation has been thought to be minimal or non-existent in these zones due to conditions unfavorable for microbial activity (Interstate Technology and Regulatory Council (ITRC) 2009a; Seagren et al. 2002). However, research has shown that biodegradation of LNAPL can occur and may be mediated by microorganisms present at the LNAPL-water interface or via the activity of excreted enzymes (ITRC 2009b; Ortega-Calvo and Alexander 1994; Zeman et al. 2014). Thus, microbially based remediation technologies are emerging for treatment of LNAPL source zones. To meet treatment goals, such technologies ideally should be developed that lead to relatively rapid biodegradation rates (i.e., that exceed natural attenuation rates) (Zeman et al. 2014). However, the fundamental microbiological processes responsible for the degradation of contaminants in LNAPL-containing zones, the key microorganisms involved, and the effects of site geochemistry on microbial communities are still not well understood. This knowledge is needed to drive development and implementation of sound remedies and to inform LNAPL longevity models to guide decision-making (Illman and Alvarez 2009). Further, detailed knowledge of the relevant microbial communities is needed to support development of culture-independent molecular tools for monitoring bioremediation in situ (Sutton et al. 2013).

Previous culture- and microcosm-based research on the biodegradation processes occurring in anaerobic hydrocarbon-contaminated environments has investigated the relationships between key microbial functions and microbial ecology, potential electron donors (i.e., contaminants) and electron acceptors, and other physical and chemical factors (Morris et al. 2012; Simarro et al. 2013; Viñas et al. 2005; Wu et al. 2008). However, the relevance of these studies to field sites has remained unknown because enriched microbial communities prevailing under controlled laboratory conditions often differ from those encountered in the field (Simarro et al. 2013). In contrast, directly analyzing in situ microbial communities at hydrocarbon-impacted sites potentially can lead to more field-relevant findings. Next-generation sequencing has enabled direct characterization of in situ microbial communities at selected hydrocarbon-contaminated sites including sub-tidal sediment, estuary sediment, a railway refueling station, and a crude-oil contaminant plume (Acosta-González et al. 2013; Fahrenfeld et al. 2014; Sun et al. 2013; Sutton et al. 2013). Studies to date have not revealed a consistent set of hydrocarbon-associated microorganisms even when redox conditions are apparently similar; rather, characterized microbial communities vary substantially within and between sites. Thus, additional studies are needed to advance our understanding of microbial communities at hydrocarbon-impacted sites. In particular, our knowledge of the structure of microbial communities in LNAPL bodies remains extremely limited.

The objectives of the present study were to advance understanding regarding how LNAPL bodies and site geochemistry influence microbial community structures in situ and to identify indigenous microorganisms potentially able to degrade hydrocarbons in LNAPL zones. The study was performed at a decommissioned refinery site located in the western USA. The refinery was active from 1923 to 1982, and thus, subsurface microbial communities have been influenced by LNAPL for nearly a century. Additionally, evidence of active biodegradation has recently been reported for this site (McCoy et al. 2014). indicating that microorganisms capable of degrading hydrocarbons in LNAPL zones are present. Based on a previous geochemical site characterization, we hypothesized the existence of multiple subsurface zones containing distinct microbial communities. Therefore, we conducted a depth-resolved characterization of the geochemical parameters and microbial communities present in the subsurface porous media (herein referred to as soil) for the LNAPL-contaminated site and in nearby uncontaminated soils. Microbial communities were characterized using quantitative molecular techniques (e.g., quantitative PCR (qPCR)) and next-generation sequencing.

Materials and methods

Site description and soil sampling

This study was conducted at a former petroleum refinery located in the western USA. While active between 1923 and 1982, the facility processed local crude oil into fuels including diesel and gasoline. The site is adjacent to a major river in an arid region. The water table in the study area fluctuates seasonally between 2.5 and 2.9 m below ground surface (bgs) (1547.2–1546.8 m elevation). Fourteen soil cores (6.4 cm in diameter) were collected at the site during the installation of 17 multilevel sampling systems (MLSs), which were used to monitor chemical constituents in the aqueous and gas phases

(Fig. S1). Soil cores were collected by direct push drilling using a Geoprobe® rig and stored in acetate sleeves (AMS Power Probes™, American Falls, ID). Immediately after collection, the cores were cut into 0.8-m sections using a circular saw and placed on dry ice to preserve geochemical conditions during transportation to the laboratory. Sections then were stored at −20 °C until further analysis. Within 3 days, the 0.8-m sections were cut into 15-cm subsections using a circular saw, and these subsections were analyzed for the composition of the soil and hydrocarbons. For core C3, microbial communities also were characterized. This core was selected for the microbial analysis for several reasons: (1) soil recovery was excellent (~90 %) with samples down to ~4 m bgs; (2) the core was in the center of the LNAPL body, and thus, the microbial communities within would not be influenced by edge effects; and (3) the geochemical characterization showed that this core was representative of the region.

Gas and water sampling and analyses

The MLSs were installed in the borings created during soil core collection (Fig. 1a). Each installed MLS consisted of six sections of 0.3-cm outside diameter Teflon® tubing bundled around a section of PVC pipe (1.3-cm inside diameter). Each MLS had a total of six sampling ports located at 0.6-m depth intervals. Three ports were located in the vadose zone, and three ports were located below the water table (Fig. S1a). Sample ports consisted of Nitex™ (HD3-10, Tetko Inc., Elmsford, NY) cloth wrapped around each piece of Teflon tubing.

For water sampling, a peristaltic pump (Cole-Parmer, Chicago, IL) was connected to each of the MLS ports located below the water table via Master Flex™ tubing (Cole-Parmer), and water was pumped to a Multi-Probe Flow Monitoring System™ (Geotech, Denver, CO). A Symphony™ pH probe (VWR, Radnor, PA), an oxidation-reduction potential (ORP) probe (model NCL-100, ORION™, ThermoScientific, Waltham, MA), and an ORION™ Five Star Plus meter (ThermoScientific, Waltham, MA) were used to measure pH and ORP (Fig. S1b). Water samples for total petroleum hydrocarbon (TPH) analysis were collected in 10-ml glass vials sealed with Teflon-lined septa and aluminum crimp caps (Fig. S1c). Water samples (10 ml) for cation and anion analysis were filtered through 0.45-μm Acrodisc™ syringe filters (PSF, Life Sciences Advanced Technologies, St. Petersburg, FL) and collected in 10-ml vials. For cation analysis, samples were preserved with 50 μl of a 70 % HNO_3 solution and sealed with Teflon-lined septa and aluminum crimp caps. To prevent oxygen exposure for anion analysis, the 10-ml glass vials were prepared in an anoxic glove box (95 % N_2 and 5 % H_2); the vials were sealed, and a syringe connected to a needle was used to draw a vacuum in the vials, such that in the field, water could be injected through the septa for anoxic water sample collection (Fig. S1c). Aqueous samples were immediately placed on ice and transported to the laboratory for further analysis.

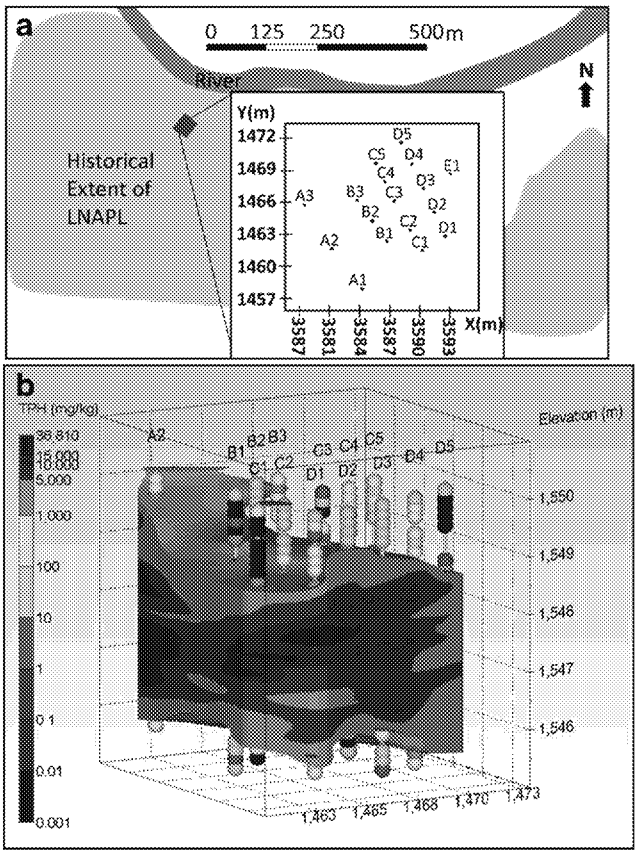

Fig. 1 **a** Plan view schematic of the field site and soil core collection and MLS locations (A1–E1). **b** TPH distribution in the surveyed LNAPL body. The nodes along the *vertical core lines* indicate the sample collection points, and the *colors* of these nodes indicate measured concentrations. Concentrations above 1000 mg/kg were considered to indicate the presence of LNAPL, and the spatial distribution of hydrocarbons in the predicted continuous LNAPL body was determined via kriging with mining visualization software, MVS™. Units along the *x*, *y*, and *z* axes are meters. Hydrocarbon concentrations are not shown for cores A1, A3, and E1 because the acetate sleeves failed during sample transport compromising the integrity of the samples from these cores

Gas samples were collected and analyzed on site for carbon dioxide, methane, and oxygen using an Eagle-2™ portable multi-gas analyzer (RKI, Union City, CA). The outlets of the sampling ports with inlets located in the vadose zone were connected to the instrument's measuring probe to collect readings. A carbon filter (Landtec, San Bernardino, CA) was utilized to remove gas phase hydrocarbons that would otherwise be detected with methane.

Hydrocarbons were extracted in methanol (core subsamples) or hexane (aqueous samples) and analyzed via gas chromatography with a flame ionization detector (FID). Cations and anions were analyzed by high-resolution inductively coupled plasma/atomic emission spectroscopy (ICP/AES)

and ion chromatography, respectively. Analytical details are provided in Supplemental Information.

Sample pretreatment and DNA extraction

The core subsamples collected for microbial characterization were stored at −20 °C until DNA extraction. To remove hydrocarbons and other potential contaminants (e.g., humic substances), which can negatively affect the DNA extraction and inhibit PCR, soil samples were pretreated as previously described (Whitby and Lund 2009) with a few modifications. For pretreatment, 120 ng of skimmed milk were added per gram of sample instead of 80 ng. In addition, polydeoxinocinic-deoxicytidilic acid was added as an aqueous solution instead of as a solid, and the sample combined with the polydeoxinocinic-deoxicytidilic solution, the skimmed milk, and 1 ml of distilled water was vortexed (1 min) and centrifuged (5000 rpm for 1 min) prior to proceeding with the wash steps as indicated by the published protocol. DNA was extracted from the pretreated samples using the PowerLyzer™ PowerSoil® DNA Isolation Kit (MoBio, Carlsbad, CA) per the manufacturer's instructions with the following modifications. To maximize DNA yield, 0.5 g of material was used for each extraction instead of 0.25 g, and duplicate DNA extractions for each sample were pooled and processed with a single PowerSoil® spin filter. Additionally, DNA was eluted with 50 to 60 μl of elution buffer instead of 100 μl to increase the DNA concentration. DNA was quantified via optical density at 260 nm with a Gen5™ Biotek microplate reader using a Take 3™ microplate (Biotek, Winoosky, VT). DNA was extracted in triplicate from each core subsample and stored at −20 °C prior to qPCR and pyrosequencing analysis.

qPCR assays

SYBR Green™ (Life Technologies, Grand Island, NY) qPCR assays were used to quantify the bacterial and archaeal 16S ribosomal ribonucleic acid (rRNA) genes. Genomic DNA extracted from *Thauera aromatica* (American Type Culture Collection (ATCC) no. 7002265D) and *Methanosarcina acetivorans* (ATCC no. 3595) was used to generate calibration curves for the bacterial and archaeal assays, respectively. The primer sets 1369F/1541r and 931AF/1100Ar were used for amplification of bacterial and archaeal 16S rRNA genes, respectively (Suzuki et al. 2000). All assays were performed using an ABI 7300 real-time PCR system (Applied Biosystems, Foster City, CA). Each 25-μl SYBR Green™ qPCR reaction contained 1× Power SYBR Green™ (Life Technologies, Grand Island, NY), forward and reverse primers (2.5 μM), magnesium acetate (10 μM), PCR grade water, and 1 ng of DNA template (based on OD_{260}). Thermocycling conditions were as follows: 95 °C for 10 min, followed by 40 cycles of 95 °C for 45 s, 56 °C for 30 s, and 60 °C for 30 s. Dissociation curve analysis was conducted to confirm amplicon specificity.

Pyrosequencing

Sample triplicates were pooled to provide sufficient DNA and generate more representative samples; pooled triplicates were sequenced as a single sample. These pooled samples were submitted to Research and Testing Laboratory, LLC (Lubbock, TX) for analysis of microbial communities using a Genome Sequencer FLX Plus 454™ Pyrosequencer (Roche, Indianapolis, IN). The primer sets 939f/1492r and 341f/1492r were used for bacterial and archaeal communities, respectively. DNA amplicons were pyrosequenced from the 5′ end. Pyrosequencing data analysis was performed by Research and Testing Laboratory, LLC, as previously described (Zeman et al. 2014). or OTU selection and classification were conducted as described by Edgar (2010). These sequence data have been submitted to GenBank databases under accession number PRJNA272921.

Data analysis

Geochemical data were visualized utilizing MVS™ (Mining Visualization System) software (C Tech Development Corporation, Henderson, NV). Measured soil and aqueous phase constituent concentrations at specific locations are represented as nodes along the vertical lines in Figs. 1, 2, and 3. Predicted constituent distributions were generated by kriging measured concentration data. For kriging calculations, non-detects were represented in MVS™ as concentrations of 0.001 mg/kg (soil) and 0.001 mg/l (aqueous). Thus, hydrocarbon or geochemical constituent concentrations shown as 0.001 mg/kg or mg/l in Figs. 1, 2, and 3 were actually below the detection limit. Indicator kriging was used to create the geology subsurface model.

Shannon diversity indexes (H′) were calculated for each sample using genus-level data (DeJong 1975). To analyze similarities between microbial communities, pyrosequencing data were used to construct community Bray-Curtis similarity matrices, and non-metric multidimensional scaling (MDS) plots were generated using Primer V6 (Primer-E Ltd., Plymouth, UK) (Clarke 1993). Stress values were calculated and indicated reliable ordinations (Clarke 1993). Histograms were generated to display genus-level microbial community composition and putative functions. To highlight groups of microorganisms shown to share functional capabilities, putative nitrate reducers, iron reducers, sulfate reducers, and methane oxidizers were reported as groups. Genera included in each group are provided in Supplemental Information.

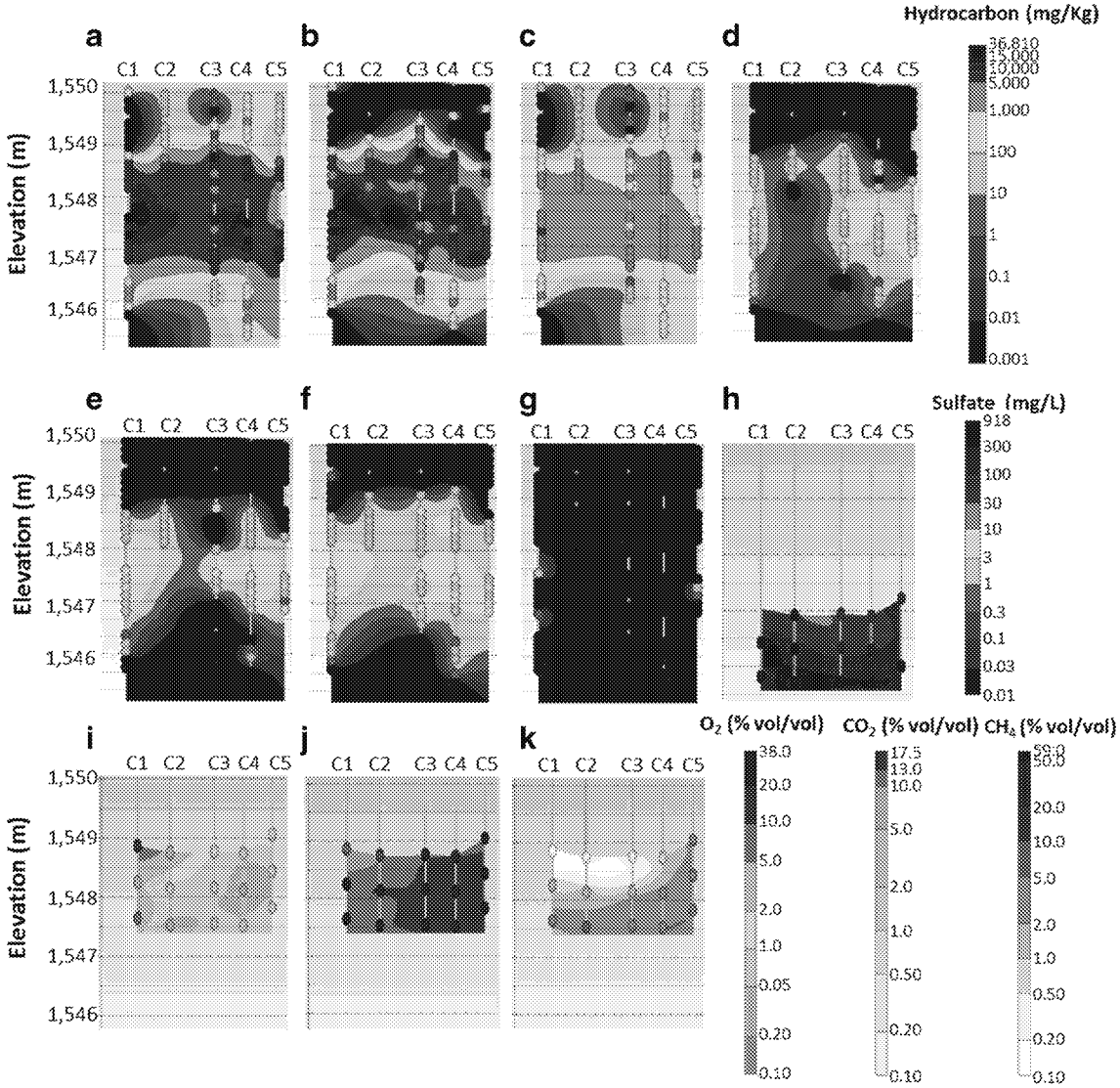

Fig. 2 Contaminant depth distribution in soil cores, aqueous phase sulfate, and gases along the C transect. Aqueous concentrations were measured in water sampled from three MLS ports located below the water table. Partial pressures were measured in gas sampled from three MLS ports located above the water table. Gas results are reported in % *v/v*. Toluene was not detected. Water samples could not be recovered from the MLS for C1 at 1547.0 m elevation, for C4 at 1545.1 m, or for C5 at 1545.7 m. **a** TPH. **b** DRO. **c** GRO. **d** Benzene. **e** Ethylbenzene. **f** *m*-Xylene and *p*-xylene. **g** *o*-Xylene. **h** Sulfate. **i** Oxygen. **j** Carbon dioxide. **k** Methane. All figure panels are available individually in Supporting Information along with soil geologic composition, measured aqueous concentrations of hydrocarbons, nitrate, ORP, and pH (Figs. S2–S20)

Results

Geochemical characterization of the LNAPL body

Site geology, hydrocarbons, and potential electron acceptors were examined above, within, and below the LNAPL body. Sands and silts dominated in the surveyed region (Fig. S2). Hydrocarbons were detected between 0.2 and 4.9 m bgs (1549.9–1544.8 m elevation), and the LNAPL body was located approximately between 0.9 and 3.7 m bgs (Figs. 1 and 2 and Fig. S3). Hydrocarbons extended well above and below the water table, which fluctuates at the site approximately between 2.5 and 2.9 m bgs (1547.2 to 1546.8 m elevation). The average TPH concentration within the LNAPL body was 8100 mg/kg (±6300). The average of the maximum TPH concentrations within each core was 17,800 mg/kg (±8200 mg/kg), and the average depth where these maximum concentrations were recorded was above the water table at ~1547.8 (±0.49)m elevation.

The majority of the hydrocarbon mass (>80 %) present was diesel range organics (DROs; Fig. 2b and Fig. S4). The highest DRO concentrations (>1000 mg/kg) were found between 0.9 and 3.7 m bgs (~1548.8 to 15445.8 m elevation), with the exception of a single high DRO concentration

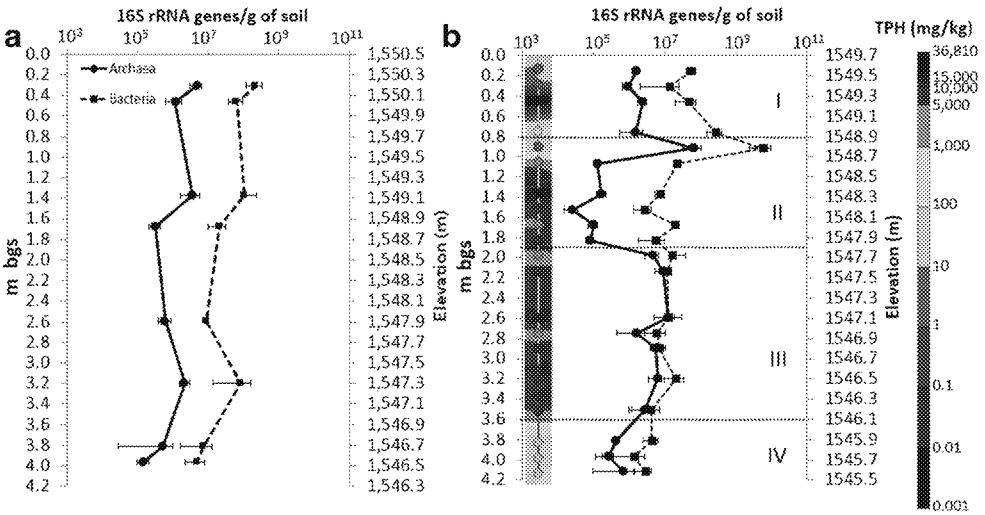

Fig. 3 Quantities of 16S rRNA genes for bacteria (*dashed line*) and archaea (*solid line*) along the central core (C3). The *error bars* correspond to standard deviations for qPCR reactions run on DNA extracted from triplicate soil samples. TPH concentrations for core C3 are included on the *left of the graph* to facilitate comparisons

(25,332 mg/kg) detected in A2 at 0.8 m bgs. Little (<1000 mg/kg) or no DRO was found closer to the surface. Gasoline range organics (GROs) were detected in substantially lower concentrations than DRO, but the depth distribution of GRO was similar to that observed for DRO (Fig. 2c and Fig. S5). Benzene, ethylbenzene, and *m*-xylene and *p*-xylene also were detected in soil cores between 0.2 and 4.4 m bgs (1549.5 to 1545.3 m elevation) and in aqueous samples (Fig. 2d–g and Figs. S6–S11). By contrast, *o*-xylene was detected only at low levels (<34 mg/kg) in a few samples (13 out of 252 in soil cores) (Fig. S12) and was not detected in any aqueous samples. Toluene was not detected in any of the soil or water samples (305 samples assayed). The relatively low levels of GRO and absence of toluene, combined with recently published data showing higher CO_2 fluxes at grade compared to nearby uncontaminated locations (McCoy et al. 2014). indicated ongoing microbial degradation.

Redox conditions were evaluated via measurement of ORP, nitrate, ferrous iron, and sulfate. The saturated region was a reducing environment (ORP values ranged from −225 to −325 mV [Ag-AgCl]) with a neutral pH (values ranged between 6.95 and 7.30) (Figs. S13 and S14). ORP and pH values were not available for the vadose zone because ORP and pH were measured only in aqueous samples. Aqueous nitrate concentrations were generally low (<1 mg/l for C transect and less than 2.5 mg/l for the whole surveyed region) (Fig. S16). Total dissolved iron concentrations also were generally low (<1 mg/l for C transect and less than 25 mg/l for the whole surveyed region) (Fig. S17). In contrast, relatively high levels of aqueous sulfate were detected; along transect C, sulfate values ranged from 45 to 726 mg/l (Fig. 2h and Fig. S15). High sulfate content in soils is common in the site climatic region and is likely due to a history of low-precipitation and high-evaporation rates. Further, sulfate gradients were observed with the highest sulfate values recorded at greater depths (below ~4.0 m bgs; 1545.7 m elevation). Additionally, black precipitate characteristics of metal sulfides were observed on the soils.

Characterization of gases in the vadose zone

Oxygen, carbon dioxide, and methane were detected in vadose zone gas samples. Oxygen concentrations ranged from 0.2 to 13.0 % (*v*/*v*), with the highest oxygen concentrations for each core (0.5 to 13.0 %*v*/*v*) occurring at the top of the sampled region (~1.1 m bgs; 1548.6 m elevation) (Fig. 2i and Fig. S18). Oxygen concentrations were presumably higher above 1.1 m bgs; however, values were not available above this depth because sampling ports were positioned strategically within the LNAPL body. Carbon dioxide and methane gas concentrations followed expected opposite trends, with higher concentrations of carbon dioxide and methane observed at locations where oxygen levels were lower (Fig. 2j, k and Figs. S19 and S20). Carbon dioxide levels along transect C ranged from 4.7 to 15.4 %*v*/*v*, and methane levels ranged from non-detect in the shallowest sample location in C1 to 5 %*v*/*v* at deeper locations (Fig. 2j, k). Thus, evidence of methanogenesis and hydrocarbon mineralization was observed, and aerobic processes likely only played a major role above 1.4 m bgs (1548.3 m elevation).

Quantification of bacteria and archaea

qPCR revealed that in general, quantities of bacteria and archaea were similar in the LNAPL body and in a nearby uncontaminated control core (Fig. 3). In the uncontaminated core, the levels of archaea were found to be approximately 5 to 50 times lower than the levels of bacteria (i.e., 2–16 % of the microbial community) at all depths based on quantities of 16S rRNA genes, as has been reported previously (Bates et al. 2011). In the contaminated core, the relative quantities of bacteria and archaea differed as a function of depth. In the upper

vadose zone (~0–0.8 m bgs), the average quantity of bacterial 16S rRNA genes was 9.6×10^7, and in this zone, the average quantity of archaeal 16S rRNA genes was 60-fold lower at 1.6×10^6 (Fig. 3). This trend held for the upper portion of the LNAPL body (~0.9–1.9 m bgs). The average quantities of bacterial and archaeal 16S rRNA genes were generally lower in the upper portion of the LNAPL body than above it, with the exception of the top of the LNAPL body (~0.9 m bgs). For the lower part of the LNAPL body (~2.0–3.6 m bgs), the average quantity of archaeal 16S rRNA genes was found to be about 60 times higher than in the upper part, excluding 0.9 m bgs. Further, the quantities of archaeal and bacterial 16S rRNA genes were approximately equal. This relationship also was observed below the LNAPL body (3.7–4.1 m bgs), where hydrocarbons were dissolved.

Microbial community characterization

After quality control and chimera removal, a total of 283,618 reads were obtained for the contaminated and clean cores collectively, representing 146,847 unique sequences. For the bacterial pyrosequencing, the average number of high-quality, chimera-free reads was 10,600 per DNA extract and the range was 1200–44,000 reads per extract. For the archaeal pyrosequencing, the average number of high-quality, chimera-free reads was 3600 per DNA extract and the range was 1100–8300 reads per extract. The average length for the unique sequences was 492 base pairs with a standard deviation of 53 base pairs. In the contaminated core, bacterial communities were dominated by seven phyla (i.e., these phyla each represented at least 5 %) and archaeal communities were dominated by two phyla (data not shown). Bacterial phyla included *Acidobacteria*, *Actinobacteria*, *Bacteroidetes*, *Chloroflexi*, *Firmicutes*, *Proteobacteria*, and *Synergistetes*, while archaeal phyla included *Euryarchaeota* and *Thaumarchaeota*. In the clean core, bacterial communities were dominated by five phyla including *Acidobacteria*, *Actinobacteria*, *Firmicutes*, *Nitrospirae*, and *Proteobacteria*. Archaeal communities were dominated by *Thaumarchaeota*.

16S rRNA gene amplicon pyrosequencing revealed that microbial community structures were distinct between the contaminated and uncontaminated control cores and varied with depth in the contaminated core (Fig. 4). An MDS plot for the bacterial communities revealed that bacterial communities in the contaminated core formed three clusters at the 40 % similarity level: (1) communities at the top of the vadose zone (samples from 0.3 to 0.5 m bgs), (2) communities in the top of the LNAPL body (samples from 1.4 to 1.7 m bgs), and (3) communities in the bottom of the LNAPL body and just below the LNAPL body (samples from 2.0 to 4.1m bgs). Bacterial communities observed in the highest part of the LNAPL body (samples from 0.9 to 1.1 m bgs) did not cluster with any other bacterial communities at the 40 % similarity level but were generally closer to other communities in the top of the LNAPL body than to any other communities. Bacterial communities from the uncontaminated core formed a distinct cluster at the 60 % similarity level, with the exception that the community observed at 0.3 m bgs in the contaminated core clustered with the communities from the uncontaminated core. Further, in the top of the vadose zone, where LNAPL was not observed and where contaminant concentrations were relatively low (<9.3 mg/kg), microbial communities were similar at the 40 % level between the contaminated and uncontaminated cores.

An MDS plot of archaeal communities (Fig. 4b) revealed that archaeal communities in the contaminated core formed the same three main clusters that were observed for bacterial communities at the 40 % similarity level, with the exception that the communities observed at 0.9–1.4 m bgs formed a tight cluster, while the community observed at 1.7 m bgs clustered with communities in the bottom of and just below the LNAPL body. Similar to communities observed for bacteria, archaeal communities in the uncontaminated core formed a completely distinct cluster, with the exception that the community observed at 0.3 m bgs clustered with communities observed in the top of the vadose zone in the contaminated core.

Interestingly, bacterial community diversity was found generally to increase in the subsurface regions impacted by high levels of hydrocarbons (i.e., 0.9 m bgs and below) as compared to the uncontaminated core (Tables S1–S5). Shannon diversity values ranged from 1.46 to 2.08 in the uncontaminated core (average of 1.64±0.19), while values ranged from 1.78 to 3.93 (average of 2.99±0.7) for the contaminated core. Similar trends were observed for archaea. However, a relative loss of bacterial diversity was observed for samples between 2.6 and 3.5 m bgs as compared to the rest of the samples impacted by moderate to high levels of hydrocarbons, and archaeal diversity was lower from 2.0 to 4.1 m bgs as compared to shallower depths.

Genus-level analysis showed that bacterial communities in the clean core were dominated by *Acidobacterium* and *Holophaga* (Fig. 5a). These same genera were predominant in the contaminated core above the LNAPL body, along with *Conexibacter* and *Bacillus* (Fig. 5c). In the top of the LNAPL body, bacterial community structures were highly variable; dominant genera included those associated with reduction of sulfate, iron, and nitrate as well as *Hydrogenophilus*, *Lysobacter*, *Thiobacillus*, *Bacillus*, *Bacteroides*, *Koribacter*, *Clostridium*, *Thermoanaerobacterium*, *Thermoanaerobacter*, and *Synergistes*. Methane oxidizers were also observed at 1.1 m bgs. By contrast, the bottom of the LNAPL body and just below the LNAPL body largely were dominated by *Syntrophus*. However, putative sulfate and iron reducers, *Acinetobacter* and *Synergistes*, also were observed. Archaeal communities in the clean core were dominated by *Nitrososphaera* and *Cenarchaeum*. Similarly, *Nitrososphaera*

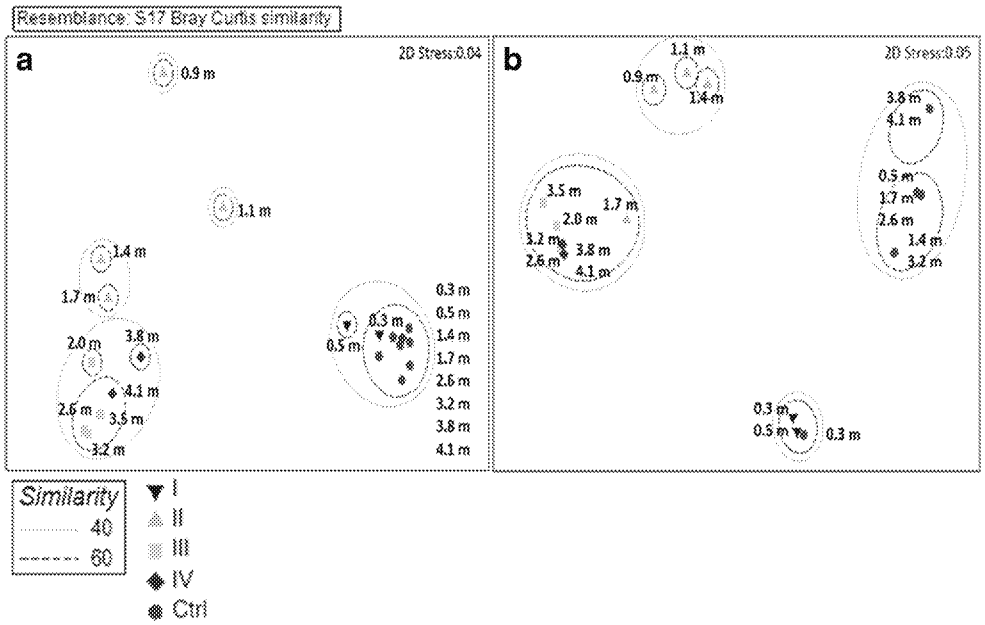

Fig. 4 Non-metric multidimensional scaling plots based on 454 pyrosequencing data for bacteria (**a**) and archaea (**b**). Labels for the control core in **a** are all shown to the *right of the plotted points* for readability

were dominant in clean cores above the LNAPL body. In the top of the LNAPL body, methanogens were observed including *Methanobrevibacter*, *Methanocella*, *Methanosaeta*, *Methanolinea*, *Methanosphaera*, and *Methermicoccus* (Evans et al. 2009; Narihiro and Sekiguchi 2011). In the bottom of the LNAPL body and just below the LNAPL body, *Methanosaeta* and *Methanoculleus* dominated.

Discussion

To advance our understanding of the microorganisms that drive microbially mediated processes in LNAPL bodies, a depth-resolved characterization of the geochemical parameters and microbial communities present at an LNAPL-impacted site was conducted. Microbial quantification suggested that during the preceding century of LNAPL influence, LNAPL-tolerant microbial communities have been established and microorganisms present readily grow in the presence of LNAPL (Fig. 3). Further, major shifts in both bacterial and archaeal community structures were found at the LNAPL-impacted location. Generally, this shift in community structure coincided with an increase in community diversity. These findings are consistent with the observations of dos Santos et al. (2011). who observed an increase in diversity 23 days after microbial communities were exposed to hydrocarbons via pyrosequencing. The increase in bacterial diversity is likely due to the presence of hydrocarbons with diverse structures as previously suggested (dos Santos et al. 2011) and potentially diverse redox niches (e.g., aerobic, sulfate-reducing, and methanogenic). By contrast, diversity decreased in the region within the LNAPL body that was below the water table. Similarly, Sutton et al. (2013) observed a decrease in microbial community diversity at a site that had been impacted by diesel hydrocarbons for over 40 years. Thus, observed lower-diversity regions are likely the result of nearly a century of selective ecological pressures and potentially more restrictive redox conditions (dominant methanogenic conditions). However, further investigations are required to clarify the driving factors leading to opposite trends in microbial diversity above and below the water table.

Quantities of bacterial and archaeal 16S rRNA genes and MDS analysis coupled to the depth-resolved geochemical data suggested that the subsurface could be conceptualized as containing four distinct biogeochemical zones (Figs. 3, 4, and 5). The top of the vadose zone (zone I, between 0 and 0.8 m bgs [~1549.7–1548.9 m elevation]) did not contain LNAPL and had low hydrocarbon concentrations; the average TPH concentration for 65 samples was 196.2 mg/kg (±364.3 mg/kg), excluding one anomalously high sample collected at 0.8 m bgs in core A2. Zone I was presumably aerobic, given that oxygen was detected below this zone at ~1.1 m bgs (1548.6 m elevation) and aerobic organisms dominated. *Acidobacterium* spp. (Ward et al. 2009) represented 34.5–63.5 % of bacterial communities, and collectively, *Nitrososphaera* spp. and *Candidatus Nitrososphaera* spp. (Jung et al. 2011; Zhalnina et al. 2014) represented over 90 % of the archaea present. Generally, phylotypes observed were similar to those in the uncontaminated core in this zone (Fig. 5 and Supplemental Tables S1 and S5). Interestingly, bacteria previously associated with aerobic hydrocarbon degradation (e.g., *Holophaga*, *Bacillus*, and low levels of *Pseudomonas* [0.2 %]) were observed (Fig. 5) (Abed et al. 2002; Ghazali et al. 2004). Thus, hydrocarbon degradation may be occurring in zone I via aerobic pathways. However, further studies (e.g., with RNA-based tools targeting functional genes) would be needed to test this hypothesis.

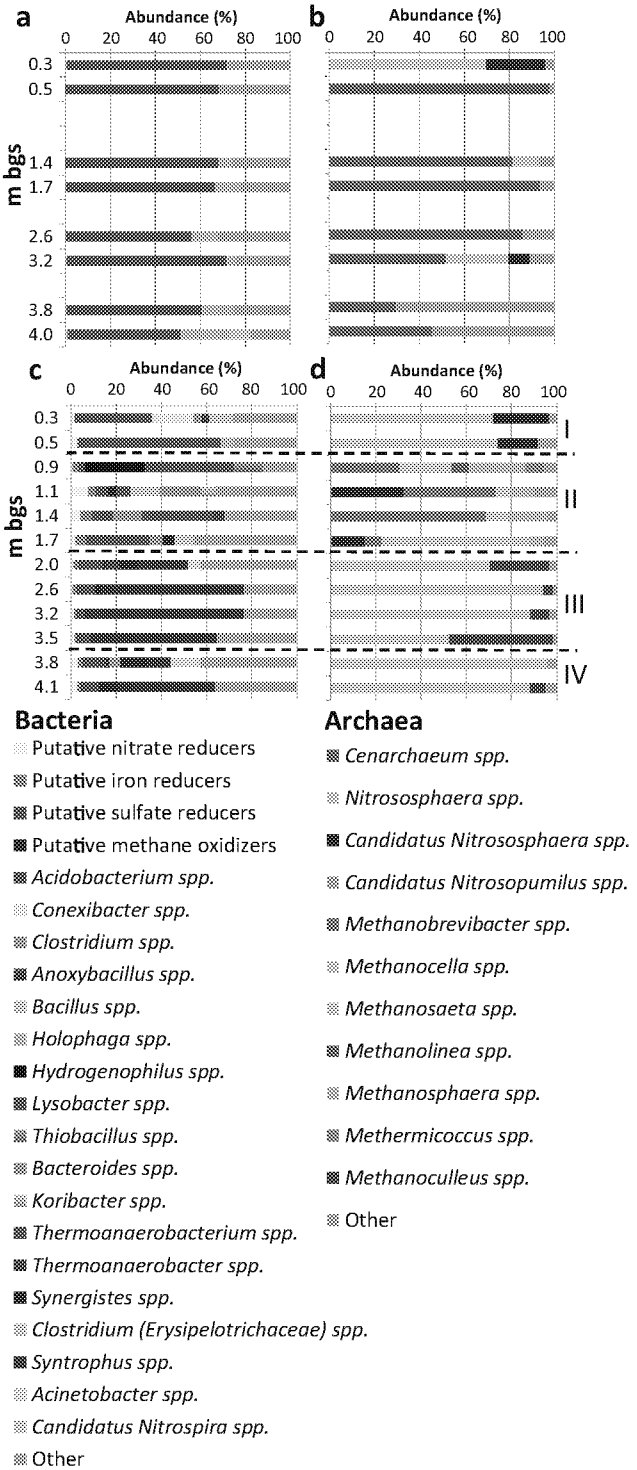

Fig. 5 Genus-level microbial community analysis with depth based on 454 pyrosequencing. Relative abundances are provided in Tables S1–S5. Histograms are shown for bacteria (**a**) and archaea (**b**) in the uncontaminated core and for bacteria (**c**) and archaea (**d**) in the LNAPL-impacted core. To highlight groups of microorganisms that have been shown to share functional capabilities, putative nitrate reducers, iron reducers, sulfate reducers, and methane oxidizers were reported as groups. Genera not associated with these functional groups and that represented less than 3 % of the microbial communities were combined and reported as "other"

The top of the LNAPL body (zone II, between 0.9 and 1.9 m bgs [~1548.8–1547.8 m elevation]) contained high contaminant concentrations (6503.6 mg/kg [±5632.3.3 mg/kg]) and was entirely above the water table. Collectively, findings suggest that zone II functions as a transition zone between the aerobic and anaerobic zones. The lack of a tight cluster for microbial communities in this zone indicates that community structures change substantially as a function of depth due to changes in redox conditions. Low levels of oxygen penetrate this zone. The peak in microbial quantities at 0.9 m bgs (Fig. 3) is likely explained by the presence of high levels of hydrocarbons coupled with the presence of oxygen; indeed, genera associated with aerobic hydrocarbon degradation were observed, albeit at low levels (e.g., *Pseudomonas* [0.2 %] and *Acidovorax* [0.09 %]) (Aburto and Peimbert 2011; Huang and Li 2014; Karimi et al. 2015; Polissi et al. 1990; Salamanca and Engesser 2014; Singleton et al. 2009; Worsey and Williams 1975). Oxygen penetration also supports methane oxidation at the top of this zone; the highest relative percent of methane oxidizers (3.7 %) was at ~1.1 m bgs (Fig. 5c). Additionally, communities were rich in facultative, fermenting microorganisms such as *Lysobacter* and *Bacillus* (39.9 and 13 %, respectively) (Glatz and Goepfert 1976; Roh et al. 1992). However, the subsurface becomes anaerobic (i.e., below ~1.4 m bgs) as available oxygen is utilized for the aforementioned processes. Further, methane production in this zone and upward flux of methane from deeper zones likely contribute to promoting anaerobic conditions in zone II by limiting the downward flux of oxygen. Bacteria previously characterized as facultative fermenters or previously associated with reduction of sulfate, iron, and nitrate were prominent in zone II. High levels of thiosulfate reducers associated with sulfur and iron cycles, such as *Thermoanaerobacterium* spp. (31.4 %) and *Thermoanaerobacter* spp. (5.2 %) (Ravot et al. 1995). were found at the center of this zone (1.4 m bgs). *Thermoanaerobacterium* spp. may be contributing to hydrocarbon degradation and producing hydrogen as they have been observed in oil phase reservoir fluids (Wang et al. 2014) and an oil reservoir flow pipeline (Singh et al. 2014). The deepest sample (1.7 m bgs) contained the highest percentage of putative sulfate-reducing microorganisms within zone II (28.0 %), most of which (90.0 %) were identified as *Desulfovibrio* spp. (Hao et al. 1996). *Clostridium* spp. (5.3 %), *Clostridium* (*Erysipelotrichaceae*) spp. (8.4 %), and *Synergistes* spp. (5.7 %) also were identified. Although these genera have been associated with sulfate reduction, they are more aptly considered facultative fermenters and are likely involved in organic acid fermentation with the generation of hydrogen, acetate, and carbon dioxide (Sieber et al. 2012). This metabolic pathway is possible in syntrophic association with hydrogenotrophic methanogens that serve as an electron sink for produced H_2, which were observed starting in zone II (Fig. 5d). Consistent with zone II being a transition zone,

Methanobrevibacter spp., which are known to tolerate low oxygen levels (Jennings et al. 2014). are prevalent at the top of this zone (0.9–1.4 m bgs), while *Methanosaeta* spp., which are known to be oxygen intolerant, were found to dominate at the bottom (Fig. 5d). Given that the study reported herein used DNA-based methods only, determining which metabolic processes are taking place is not possible; however, the presence of both hydrogenotrophic and acetoclastic methanogens also suggests that syntrophic degradation processes were occurring in the lower part of zone II (Plugge et al. 2011).

Additionally, zone II could potentially be characterized by regions with elevated temperatures. Methane oxidation is known to be a highly exothermic process (Haynes and Gonzalez 2014). and heat produced may result in increased temperatures in the surrounding soils. The observed high levels of *Thermoanaerobacterium* spp. (31.4 %) and *Thermoanaerobacter* spp. (5.2 %) below the methane oxidation hot spot provide a line of evidence that methane oxidation may result in substantive temperature increases as these genera are known to be thermophilic (Fardeau et al. 2000; Roy et al. 2014). Increased subsurface temperatures due to methane oxidation remain a hypothesis requiring further experimentation; however, such a finding would have bearing on kinetics of hydrocarbon degradation and methanogenesis. Heat produced from methane oxidation has been shown to increase methane production, and temperature increases have been shown to increase hydrocarbon degradation rates (Zeman et al. 2014). Temperature also has been shown to be a key factor in determining microbial community structure, which may influence degradation rates (Zeman et al. 2014).

Interestingly, MDS analysis (Fig. 4) suggested that the bottom of the LNAPL body (2.0 - 3.6 m bgs [~1547.7–1546.1 m elevation]) is a distinct zone (III), despite containing similar levels of hydrocarbons to zone II (9556.5 mg/kg [±7286.1]), because bacterial communities observed formed a tight cluster and were distinct from communities in other zones (Fig. 5). The water table was found to be between 2.5 and 2.9 m bgs [1547.2–1546.8 m elevation] for the contaminated core, and taking into account water table fluctuations and the capillary fringe, zone III is largely either saturated or characterized by high moisture content (e.g., in the capillary fringe). High moisture content generally results in reduced oxygen levels (Hers et al. 2014). These factors may explain why observed microbial communities in zone III were distinct from those observed in zone II.

In zone III, bacterial communities were found to be dominated by species identified as *Syntrophus* spp., which have been linked to anaerobic hydrocarbon degradation (McInerney et al. 2007; Mountfort et al. 1984; Siddique et al. 2011). This zone also contained other phylotypes that may be implicated in hydrocarbon degradation. *Pelotomaculum* spp., which were found both above and below the water table in the contaminated core but not in the uncontaminated core, have been associated specifically with anaerobic benzene degradation (Kleinsteuber et al. 2008, 2012; Vogt et al. 2011). *Desulfosarcina*, *Desulfotomaculum*, and *Desulfoporosinus* also were found, and these genera may be involved in fermentation as sulfate gradients suggested that sulfate concentrations are low in zone III. Moreover, *Pelotomaculum*, *Desulfotomaculum*, and *Desulfoporosinus* are all members of the *Peptococcaceae* family, which has been linked with the initial steps in anaerobic benzene degradation (Abu Laban et al. 2010; Luo et al. 2014). Further, archaeal quantities showed that archaea-driven processes (i.e., methanogenesis) play a more significant ecological role in the lower portion of the LNAPL body than in the upper portion, despite anaerobic conditions throughout the LNAPL body (Fig. 3). Collectively, *Methanosaeta* spp. (acetoclastic) and *Methanoculleus* spp. (hydrogenotrophs) account for over 90 % of the archaea detected within zone III. These two methanogenic genera have been reported to predominate in environments where syntrophic hydrocarbon degradation occurs (Kleikemper et al. 2005; Liu et al. 2009). Thus, relatively high levels of archaea, specifically *Methanoculleus* (e.g., 46.1 % at 3.5 m bgs; Fig. 5d), coupled with detection of methane and low ORP, provide lines of evidence that suggest that methanogenesis is a dominant process in zone III.

The surveyed region below the LNAPL body (between 3.7 and 4.9 m bgs [~1546.0–1544.8 m elevation]) was conceptualized as a distinct zone, zone IV, despite similar microbial communities to zone III because this zone contained low levels of hydrocarbons (2117.8 mg/kg [±2825.9]); in core C3, where the microbial community analysis was conducted, TPH ranged from only 24 to 90 mg/kg. This zone also contained relatively high levels of sulfate (up to 852 mg/l). The observed sulfate gradient (Fig. 2h and Fig. S15), along with black soil precipitate characteristic of metal sulfides and the presence of sulfate-reducing bacteria (Fig. 5c), suggests that sulfate reduction is an important process in zone IV. The archaeal communities in zone IV were composed mainly of *Methanosaeta* spp., and *Methanoculleus* spp. (7.2 %) were only found at 4.1 m bgs. In areas where sulfate reduction is a dominant process, hydrogenotrophic organisms like *Methanoculleus* spp. may be outcompeted by sulfate-reducing organisms which act as hydrogen scavengers. However, although no gas samples could be recovered within zone IV (because it is below the water table), methanogenesis may well be occurring simultaneously with sulfate reduction in this zone via acetoclastic pathways. Co-occurrence of methanogenesis and sulfate reduction is not unexpected as heterogeneity in the subsurface is high, and the presence of multiple microbial guilds in close proximity has been reported previously (Tischer et al. 2013; Winderl et al. 2008).

The presence of distinct microbial phylotypes in the contaminated core as compared to the clean core, coupled with recently published data indicating that hydrocarbon

degradation is actively occurring at the site studied herein (McCoy et al. 2014). provides evidence linking observed microbial phylotypes with hydrocarbon degradation processes within the LNAPL body. *Syntrophus*-related species were not detected in the clean core, while they represented between 10 and 70 % of the bacterial communities in zones III and IV (Fig. 5). Interestingly, greater than 80 % of the 16S rRNA gene sequences identified as *Syntrophus* spp. were found to be most similar (≥97 %) to a strain (clone B3) derived from a methanogenic culture enriched on hexadecane by Zengler et al. (1999). Additionally, the highest level of benzene detected in the contaminated core soil (2.6 m bgs; Fig. 2d) coincided with the second highest detected percent of *Syntrophus* spp. (63.6 %; Fig. 5c). In culture-based studies, members of this genus have been shown to syntrophically degrade benzoate (Jackson et al. 1999; Mountfort et al. 1984). which is likely produced via the first step in anaerobic benzene degradation (Luo et al. 2014; Vogt et al. 2011). and to syntrophically degrade other organic acids to acetate and hydrogen. *Syntrophus* spp. also have been associated with anaerobic degradation of petroleum liquids, such as cyclohexane (Elshahed et al. 2001; McInerney et al. 2007; Siddique et al. 2011) and hexadecane (Zengler et al. 1999). Additionally, a strain related to *Syntrophus* spp. Hasda-A was reported to be the most prominent bacterium that assimilated stable isotope-labeled benzene in a benzene-degrading, methanogenic culture derived from lotus field soil (Sakai et al. 2009). Thus, past culture-based studies and observed high levels of *Syntrophus* spp. in the subsurface suggest that *Syntrophus* spp. may play a key role in hydrocarbon degradation in situ, and could be degrading hydrocarbons to acetate, which is subsequently used by *Methanosaeta* spp. to produce methane.

Syntrophus-related species also have been identified in clone libraries derived from a coal-tar-waste-contaminated aquifer (Bakermans and Madsen 2002) and a methanogenic zone in hydrocarbon-impacted aquifer (Dojka et al. 1998). although the relative quantity of *Syntrophus* spp. was not investigated in these studies. In a recent in situ study, Tischer et al. (2013) did not observe *Syntrophus* spp. in the capillary fringe and subjacent sediments in a hydrocarbon-contaminated aquifer, but they did observe other highly related members of the *Syntrophaceae* family (*Smithella*-related species). By contrast, *Syntrophus* spp. were not reported among the key microbial phylotypes present at a long-term diesel-contaminated site (Sutton et al. 2013). which could indicate that *Syntrophus* spp. are associated with degradation of GRO constituents rather than DRO. Alternatively, this finding could suggest that other, as yet unidentified, environmental factors play a role in selecting for high levels of *Syntrophus* spp. in the subsurface. Additionally, *Syntrophus* spp. are distinct from phylotypes that have been observed to dominate in hydrocarbon plumes where *Alphaproteobacteria* and *Betaproteobacteria* were found to dominate (Fahrenfeld et al. 2014; Winderl et al. 2008). suggesting that they may be especially well adapted to grow in LNAPL bodies. Thus, *Syntrophus* spp. likely represent useful targets for development of culture-independent molecular tools for monitoring bioremediation of LNAPL in situ (Sutton et al. 2013). Further, metagenomic sequencing targeting *Syntrophus* spp. (e.g., via single-cell sequencing (Mason et al. 2014). could potentially reveal functional gene targets ideal for monitoring bioremediation.

In summary, in this study, depth-resolved characterization of biogeochemical parameters for a shallow, hydrocarbon-impacted aquifer revealed the presence of four distinct zones: (i) an aerobic, low-contaminant mass zone at the top of the vadose zone; (ii) a moderate to high-contaminant mass, low-oxygen to anaerobic transition zone in the middle of the vadose zone; (iii) an anaerobic, high-contaminant mass zone spanning the bottom of the vadose zone and saturated zone; and (iv) an anaerobic, low-contaminant mass zone below the LNAPL body. Data indicated that in the lower part of zone II and in zone III, hydrocarbon degradation was mediated largely by syntrophic fermenters and methanogens. Although zone II was completely above the water table, anaerobic conditions were observed in the lower portion of this zone likely, in part, because produced methane limited downward diffusion of oxygen. Zone IV was influenced by high levels of sulfate, and sulfate reduction, in addition to methanogenesis, was likely a key driver of hydrocarbon depletion at the bottom of and below the LNAPL body. Pyrosequencing data revealed potential targets for development of molecular tools for monitoring bioremediation in situ, and findings reported herein represent the first data showing the dominance of *Syntrophus*-related species in an LNAPL body where active degradation is occurring. Future work should focus on resolving the activities of observed phylotypes in the presence of LNAPL.

Acknowledgments Funding for this work was provided by Chevron, Exxon Mobil, and the National Science Foundation via an Alliance for the Graduate Education and Professoriate (AGEP) fellowship awarded to M. Irianni - Renno. The authors would like to thank site consultants from TriHydro Inc., Alysha Hakala, Thomas Gardner, Stephanie Whitfield, Shawn Harshman, and Ben McAlexander, for their technical support in the field.

Compliance with ethical standards This article does not contain any studies with human participants or animals performed by any of the authors.

Funding This study was funded by Chevron and Exxon Mobil and by the US National Science Foundation via an Alliance for the Graduate Education and Professoriate (AGEP) fellowship awarded to M. Irianni - Renno.

Conflict of interest M. Irianni - Renno declares she has no conflict of interest. D. Akhbari declares he has no conflict of interest. M.R. Olson declares he has no conflict of interest. A.P. Byrne declares he has no

conflict of interest. E. Lefevre declares she has no conflict of interest. J. Zimbron declares he has no conflict of interest. M. Lyverse declares he has no conflict of interest. T.C. Sale declares he has no conflict of interest. S.K. De Long declares she has no conflict of interest.

References

Abed RMM, Safi NMD, Koster J, de Beer D, El-Nahhal Y, Rullkotter J, Garcia-Pichel F (2002) Microbial diversity of a heavily polluted microbial mat and its community changes following degradation of petroleum compounds. App Environ Microbiol 68(4):1674–1683. doi:10.1128/aem.68.4.1674-1683.2002

Abu Laban N, Selesi D, Rattei T, Tischler P, Meckenstock RU (2010) Identification of enzymes involved in anaerobic benzene degradation by a strictly anaerobic iron-reducing enrichment culture. Environ Microbiol 12(10):2783–2796. doi:10.1111/j.1462-2920.2010.02248.x

Aburto A, Peimbert M (2011) Degradation of a benzene-toluene mixture by hydrocarbon-adapted bacterial communities. Ann Microbiol 61(3):553–562. doi:10.1007/s13213-010-0173-6

Acosta-González A, Rosselló-Móra R, Marqués S (2013) Characterization of the anaerobic microbial community in oil-polluted subtidal sediments: aromatic biodegradation potential after the Prestige oil spill. Environ Microbiol 15(1):77–92

Bakermans C, Madsen EL (2002) Diversity of 16S rDNA and naphthalene dioxygenase genes from coal-tar-waste-contaminated aquifer waters. Microb Ecol 44(2):95–106. doi:10.1007/s00248-002-0005-8

Bates ST, Berg-Lyons D, Caporaso JG, Walters WA, Knight R, Fierer N (2011) Examining the global distribution of dominant archaeal populations in soil. ISME J 5(5):908–917. doi:10.1038/ismej.2010.171

Chadalavada S, Datta B, Naidu R (2012) Optimal identification of groundwater pollution sources using feedback monitoring information: a case study. Environ Forensics 13(2):140–153. doi:10.1080/15275922.2012.676147

Clarke KR (1993) Non-parametric multivariate analyses of changes in community structure. Aus J Ecol 18(1):117–143

Das N, Chandran P (2010) Microbial degradation of petroleum hydrocarbon contaminants: an overview. Biotechnol Res Int 2011. doi:10.4061/2011/941810

Declercq I, Cappuyns V, Duclos Y (2012) Monitored natural attenuation (MNA) of contaminated soils: state of the art in Europe—a critical evaluation. Sci Total Environ 426:393–405

DeJong T (1975) A comparison of three diversity indices based on their components of richness and evenness. Oikos 222–227

Dojka MA, Hugenholtz P, Haack SK, Pace NR (1998) Microbial diversity in a hydrocarbon- and chlorinated-solvent-contaminated aquifer undergoing intrinsic bioremediation. Appl Environ Microbiol 64(10):3869–3877

dos Santos HF, Cury JC, do Carmo FL, dos Santos AL, Tiedje J, van Elsas JD, Rosado AS, Peixoto RS (2011) Mangrove bacterial diversity and the impact of oil contamination revealed by pyrosequencing: bacterial proxies for oil pollution. PLoS One 6(3), e16943. doi:10.1371/journal.pone.0016943

Edgar RC (2010) Search and clustering orders of magnitude faster than BLAST. Bioinformatics 26(19):2460–2461. doi:10.1093/bioinformatics/btq461

Elshahed MS, Bhupathiraju VK, Wofford NQ, Nanny MA, McInerney MJ (2001) Metabolism of benzoate, cyclohex-1-ene carboxylate, and cyclohexane carboxylate by "*Syntrophus aciditrophicus*" strain SB in syntrophic association with H-2-using microorganisms. Appl Environ Microbiol 67(4):1728–1738. doi:10.1128/aem.67.4.1728-1738.2001

Evans PN, Hinds LA, Sly LI, McSweeney CS, Morrison M, Wright A-DG (2009) Community composition and density of methanogens in the foregut of the Tammar wallaby (*Macropus eugenii*). Appl Environ Microbiol 75(8):2598–2602

Fahrenfeld N, Cozzarelli IM, Bailey Z, Pruden A (2014) Insights into biodegradation through depth-resolved microbial community functional and structural profiling of a crude-oil contaminant plume. Microbial Ecol 68(3):453–462. doi:10.1007/s00248-014-0421-6

Fardeau ML, Magot M, Patel BKC, Thomas P, Garcia JL, Ollivier B (2000) *Thermoanaerobacter subterraneus* sp nov., a novel thermophile isolated from oilfield water. Int J Syst Evol Microbiol 50:2141–2149

Ghazali FM, Rahman R, Salleh AB, Basri M (2004) Biodegradation of hydrocarbons in soil by microbial consortium. Int Biodeterior Biodegrad 54(1):61–67. doi:10.1016/j.ibiod.2004.02.002

Glatz BA, Goepfert J (1976) Defined conditions for synthesis of *Bacillus cereus* enterotoxin by fermenter-grown cultures. Appl Environ Microbiol 32(3):400–404

Hao OJ, Chen M, Huang L, Buglass RL (1996) Sulfate-reducing bacteria. Crit Rev Environ Sci Technol 26(1):155–187

Haynes CA, Gonzalez R (2014) Rethinking biological activation of methane and conversion to liquid fuels. Nat Chem Biol 10(5):331–339

Hers I, Jourabchi P, Lahvis MA, Dahlen P, Luo EH, Johnson P, DeVaull GE, Mayer KU (2014) Evaluation of seasonal factors on petroleum hydrocarbon vapor biodegradation and intrusion potential in a cold climate. Groundw Monit Remediat 34(4):60–78

Huang YX, Li L (2014) Biodegradation characteristics of naphthalene and benzene, toluene, ethyl benzene, and xylene (BTEX) by bacteria enriched from activated sludge. Water Environ Res 86(3):277–284. doi:10.2175/106143013x13807328849495

Huntley D, Beckett GD (2002) Persistence of LNAPL sources: relationship between risk reduction and LNAPL recovery. J Contam Hydrol 59(1–2):3–26. doi:10.1016/s0169-7722(02)00073-6

Illman WA, Alvarez PJ (2009) Performance assessment of bioremediation and natural attenuation. Crit Rev Environ Sci Technol 39(4):209–270

Jackson BE, Bhupathiraju VK, Tanner RS, Woese CR, McInerney MJ (1999) *Syntrophus aciditrophicus* sp. nov., a new anaerobic bacterium that degrades fatty acids and benzoate in syntrophic association with hydrogen-using microorganisms. Arch Microbiol 171(2):107–114. doi:10.1007/s002030050685

Jennings ME, Schaff CW, Horne AJ, Lessner FH, Lessner DJ (2014) Expression of a bacterial catalase in a strictly anaerobic methanogen significantly increases tolerance to hydrogen peroxide but not oxygen. Microbiology 160(Pt 2):270–278

Jørgensen KS, Salminen JM, Björklöf K (2010) Monitored natural attenuation. Bioremediation. Springer, pp 217–233

Jung M-Y, Park S-J, Min D, Kim J-S, Rijpstra WIC, Damsté JSS, Kim G-J, Madsen EL, Rhee S-K (2011) Enrichment and characterization of an autotrophic ammonia-oxidizing archaeon of mesophilic crenarchaeal group I. 1a from an agricultural soil. Appl Environ Microbiol 77(24):8635–8647

Karimi B, Habibi M, Esvand M (2015) Biodegradation of naphthalene using *Pseudomonas aeruginosa* by up flow anoxic-aerobic continuous flow combined bioreactor. J Environ Health Sci Eng 13. doi:10.1186/s40201-015-0175-1

Kleikemper J, Pombo SA, Schroth MH, Sigler WV, Pesaro M, Zeyer J (2005) Activity and diversity of methanogens in a petroleum hydrocarbon-contaminated aquifer. Appl Environ Microbiol 71(1):149–158

Kleinsteuber S, Schleinitz KM, Breitfeld J, Harms H, Richnow HH, Vogt C (2008) Molecular characterization of bacterial communities mineralizing benzene under sulfate-reducing conditions. FEMS

Microbiol Ecol 66(1):143–157. doi:10.1111/j.1574-6941.2008.00536.x

Kleinsteuber S, Schleinitz KM, Vogt C (2012) Key players and team play: anaerobic microbial communities in hydrocarbon-contaminated aquifers. Appl Microbiol Biotechnol 94(4):851–873. doi:10.1007/s00253-012-4025-0

Landmeyer J, Chapelle F, Petkewich M, Bradley P (1998) Assessment of natural attenuation of aromatic hydrocarbons in groundwater near a former manufactured-gas plant, South Carolina, USA. Environ Geol 34(4):279–292

Liu R, Zhang Y, Ding R, Li D, Gao Y, Yang M (2009) Comparison of archaeal and bacterial community structures in heavily oil-contaminated and pristine soils. J Biosci Bioeng 108(5):400–407

Luo F, Gitiafroz R, Devine CE, Gong YC, Hug LA, Raskin L, Edwards EA (2014) Metatranscriptome of an anaerobic benzene-degrading, nitrate-reducing enrichment culture reveals involvement of carboxylation in benzene ring activation. Appl Environ Microbiol 80(14):4095–4107. doi:10.1128/aem.00717-14

Mason OU, Han J, Woyke T, Jansson JK (2014) Single-cell genomics reveals features of a *Colwellia* species that was dominant during the Deepwater Horizon oil spill. Front Microbiol 5. doi:10.3389/fmicb.2014.00332

McCoy K, Zimbron J, Sale T, Lyverse M (2014) Measurement of natural losses of LNAPL using CO_2 traps. Groundwater 53(4):658–667. doi:10.1111/gwat.12240

McInerney MJ, Rohlin L, Mouttaki H, Kim U, Krupp RS, Rios-Hernandez L, Sieber J, Struchtemeyer CG, Bhattacharyya A, Campbell JW (2007) The genome of *Syntrophus aciditrophicus*: life at the thermodynamic limit of microbial growth. Proc Natl Acad Sci U S A 104(18):7600–7605

Morris BE, Herbst FA, Bastida F, Seifert J, von Bergen M, Richnow HH, Suflita JM (2012) Microbial interactions during residual oil and n-fatty acid metabolism by a methanogenic consortium. Environ Microbiol Rep 4(3):297–306

Mountfort D, Brulla W, Krumholz LR, Bryant M (1984) *Syntrophus buswellii* gen. nov., sp. nov.: a benzoate catabolizer from methanogenic ecosystems. Int J Syst Bacteriol 34(2):216–217

Narihiro T, Sekiguchi Y (2011) Oligonucleotide primers, probes and molecular methods for the environmental monitoring of methanogenic archaea. Microbial Biotechnol 4(5):585–602

Newman WA, Kimball G, Consultants DE (1991) Dissolved oxygen mapping: a powerful tool for site assessments and ground water monitoring. In: Proceedings of the Fifth National Outdoor Action Conference on Aquifer Restoration, Ground Water Monitoring, and Geophysical Methods

Ortega-Calvo J-J, Alexander M (1994) Roles of bacterial attachment and spontaneous partitioning in the biodegradation of naphthalene initially present in nonaqueous-phase liquids. Appl Environ Microbiol 60(7):2643–2646

Plugge CM, Zhang W, Scholten JCM, Stams AJM (2011) Metabolic flexibility of sulfate-reducing bacteria. Front Microbiol 2:1–8. doi:10.3389/fmicb.2011.00081

Polissi A, Bestetti G, Bertoni G, Galli E, Deho G (1990) Genetic analysis of chromosomal operons involved in degradation of aromatic hyrocarbons in *Pseudomonas putida* TMB. J Bacteriol 172(11):6355–6362

Ravot G, Ollivier B, Magot M, Patel B, Crolet J, Fardeau M, Garcia J (1995) Thiosulfate reduction, an important physiological feature shared by members of the order *thermotogales*. Appl Environ Microbiol 61(5):2053–2055

ITRC (Interstate Technology & Regulatory Council) (2009a) Evaluating LNAPL remedial technologies for achieving project goals. LNAPL-2. Interstate Technology & Regulatory Council, LNAPLs Team, Washington, D.C. www.itrcweb.org

ITRC (Interstate Technology & Regulatory Council) (2009b) Evaluating natural source zone depletion at sites with LNAPL. LNAPL-1. Interstate Technology & Regulatory Council, LNAPLs Team, Washington, D.C. www.itrcweb.org

Roggemans S, Bruce CL, Johnson PC, Johnson RL (2001) Vadose zone natural attenuation of hydrocarbon vapors: an empirical assessment of soil gas vertical profile data. API Soil and Water Research Bulletin 15

Roh JW, Bang JH, Nam DH (1992) Nutritional requirements of *Lysobacter lactamgenus* for the production of cephabacins. Biotechnol Lett 14(6):455–460

Roy S, Vishnuvardhan M, Das D (2014) Improvement of hydrogen production by newly isolated *Thermoanaerobacterium thermosaccharolyticum* IIT BT-ST1. Int J Hydrog Energy 39(14):7541–7552. doi:10.1016/j.ijhydene.2013.06.128

Sakai N, Kurisu F, Yagi O, Nakajima F, Yamamoto K (2009) Identification of putative benzene-degrading bacteria in methanogenic enrichment cultures. J Biosci Bioeng 108(6):501–507. doi:10.1016/j.jbiosc.2009.06.005

Salamanca D, Engesser KH (2014) Isolation and characterization of two novel strains capable of using cyclohexane as carbon source. Environ Sci Pollut Res 21(22):12757–12766. doi:10.1007/s11356-014-3206-z

Sale T (2003) Answers to frequently asked questions about managing risk at LNAPL sites. API Soil and Water Research Bulletin (18): 1–20

Seagren EA, Rittmann BE, Valocchi AJ (2002) Bioenhancement of NAPL pool dissolution: experimental evaluation. J Contam Hydrol 55(1):57–85

Siddique T, Penner T, Semple K, Foght JM (2011) Anaerobic biodegradation of longer-chain n-alkanes coupled to methane production in oil sands tailings. Environ Sci Technol 45(13):5892–5899

Sieber JR, McInerney MJ, Gunsalus RP (2012) Genomic insights into syntrophy: the paradigm for anaerobic metabolic cooperation. Annu Rev Microbiol 66:429–452

Simarro R, González N, Bautista LF, Molina MC (2013) Biodegradation of high-molecular-weight polycyclic aromatic hydrocarbons by a wood-degrading consortium at low temperatures. FEMS Microbiol Ecol 83(2):438–449

Singh S, Sarma PM, Lal B (2014) Biohydrogen production by *Thermoanaerobacterium thermosaccharolyticum* TERI S7 from oil reservoir flow pipeline. Int J Hydrog Energy 39(9):4206–4214. doi:10.1016/j.ijhydene.2013.12.179

Singleton DR, Ramirez LG, Aitken MD (2009) Characterization of a polycyclic aromatic hydrocarbon degradation gene cluster in a phenanthrene-degrading *Acidovorax* strain. Appl Environ Microbiol 75(9):2613–2620. doi:10.1128/aem.01955-08

Sun MY, Dafforn KA, Johnston EL, Brown MV (2013) Core sediment bacteria drive community response to anthropogenic contamination over multiple environmental gradients. Environ Microbiol 15(9):2517–2531. doi:10.1111/1462-2920.12133

Sutton NB, Maphosa F, Morillo JA, Abu Al-Soud W, Langenhoff AAM, Grotenhuis T, Rijnaarts HHM, Smidt H (2013) Impact of long-term diesel contamination on soil microbial community structure. Appl Environ Microbiol 79(2):619–630. doi:10.1128/aem.02747-12

Suzuki MT, Taylor LT, DeLong EF (2000) Quantitative analysis of small-subunit rRNA genes in mixed microbial populations via 5′-nuclease assays. Appl Environ Microbiol 66(11):4605–4614

Tischer K, Kleinsteuber S, Schleinitz KM, Fetzer I, Spott O, Stange F, Lohse U, Franz J, Neumann F, Gerling S, Schmidt C, Hasselwander E, Harms H, Wendeberg A (2013) Microbial communities along biogeochemical gradients in a hydrocarbon-contaminated aquifer. Environ Microbiol 15(9):2603–2615. doi:10.1111/1462-2920.12168

Viñas M, Sabaté J, Espuny MJ, Solanas AM (2005) Bacterial community dynamics and polycyclic aromatic hydrocarbon degradation during bioremediation of heavily creosote-contaminated soil. Appl Environ Microbiol 71(11):7008–7018

Vogt C, Kleinsteuber S, Richnow HH (2011) Anaerobic benzene degradation by bacteria. Microbial Biotechnol 4(6):710–724. doi:10.1111/j.1751-7915.2011.00260.x

Wang LY, Ke WJ, Sun XB, Liu JF, Gu JD, Mu BZ (2014) Comparison of bacterial community in aqueous and oil phases of water-flooded petroleum reservoirs using pyrosequencing and clone library approaches. Appl Microbiol Biotechnol 98(9):4209–4221. doi:10.1007/s00253-013-5472-y

Ward NL, Challacombe JF, Janssen PH, Henrissat B, Coutinho PM, Wu M, Xie G, Haft DH, Sait M, Badger J (2009) Three genomes from the phylum *Acidobacteria* provide insight into the lifestyles of these microorganisms in soils. Appl Environ Microbiol 75(7):2046–2056

Whitby C, Lund ST (2009) Applied microbiology and molecular biology in oil field systems. Springer, Netherlands

Winderl C, Anneser B, Griebler C, Meckenstock RU, Lueders T (2008) Depth-resolved quantification of anaerobic toluene degraders and aquifer microbial community patterns in distinct redox zones of a tar oil contaminant plume. Appl Environ Microbiol 74(3):792–801. doi:10.1128/aem.01951-07

Worsey MJ, Williams PA (1975) Metabolism of toluene and xylenes by *Pseudomonas putida* (*arvilla*) mt-2: evidence for a new function of TOL plasmid. J Bacteriol 124(1):7–13

Wu Y, Luo Y, Zou D, Ni J, Liu W, Teng Y, Li Z (2008) Bioremediation of polycyclic aromatic hydrocarbons contaminated soil with *Monilinia* sp.: degradation and microbial community analysis. Biodegradation 19(2):247–257

Zeman NR, Renno MI, Olson MR, Wilson LP, Sale TC, De Long SK (2014) Temperature impacts on anaerobic biotransformation of LNAPL and concurrent shifts in microbial community structure. Biodegradation 25(4):569–585. doi:10.1007/s10532-014-9682-5

Zengler K, Richnow HH, Rossello-Mora R, Michaelis W, Widdel F (1999) Methane formation from long-chain alkanes by anaerobic microorganisms. Nature 401(6750):266–269

Zhalnina KV, Dias R, Leonard MT, de Quadros PD, Camargo FA, Drew JC, Farmerie WG, Daroub SH, Triplett EW (2014) Genome sequence of *Candidatus Nitrososphaera* evergladensis from group I.1b enriched from Everglades soil reveals novel genomic features of the ammonia-oxidizing archaea. PLoS One 9(7), e101648